Progress In Electromagnetics Research C, Vol. 39, 133–148, 2013

MULTI-BAND NOTCH UWB BAND PASS FILTER WITH NOVEL CONTIGUOUS SPLIT RINGS EMBEDDED IN SYMMETRICALLY TAPERED ELLIPTIC RINGS

Anil Kamma*, Swapnil R. Gupta, Gopi S. Reddy, and Jayanta Mukherjee

Department of Electrical Engineering, Indian Institute of Technology Bombay, Powai, Mumbai 400076, India

Abstract—A compact multiple band-notch ultra-wide band (UWB) band-pass filter (BPF) with surface area of $18 \times 12\,\text{mm}^2$ is introduced in this article. The proposed filter is a combination of novel symmetrically tapered elliptic rings (STER) and contiguous split ring resonators (SRR), with stepped impedance resonator (SIR) structure to realize the multi-band notch UWB pass band characteristics. In the proposed structure, band-notches are generated for interfering microwave bands such as, WiMAX, WLAN and X-band applications. These notches are achieved by optimizing structural parameters of SRR sections. The proposed filter is fabricated on RT/Duroid 5880 substrate with $\varepsilon_r = 2.2$ and thickness of 0.787 mm. The fabricated prototype is measured and a good agreement between simulated and measured results ensures suitability of the proposed filter for UWB applications.

1. INTRODUCTION

Due to ever increasing data rate and system compactness, there is great demand for broadband and high data rate systems. Due to its inherent properties, UWB is considered as a potential candidate for high-speed data transmission, low cost and short range indoor wireless communication systems. According to the Federal Communications Commission (FCC) guidelines [1] the bandwidth of 3.1–10.6 GHz is unlicensed, which provides a wide spectrum for component designers to achieve high level system compactness. But UWB bandwidth faces interference due to many sub communication bands such as WiMAX

Received 12 March 2013, Accepted 15 April 2013, Scheduled 18 April 2013
* Corresponding author: Anil Kamma (anilkamma@ee.iitb.ac.in).

(3.3–3.6 GHz), WLAN (5.2–5.8 GHz) and X-band applications like satellite communications (8.4 GHz) and radar systems (10 GHz), etc.. In order to avoid sub band interference, it is important that the UWB system should posses a multi-band reject filter characteristic for interfering microwave bands [2–4].

In the last couple of years there has been an extensive study on UWB RF components especially passive filters, as they play a key role in deciding system response, size and cost effectiveness. Various techniques have been reported to realize the UWB band pass filter [4, 5]. Multiple-mode resonator (MMR) with stepped impedance has been used to achieve required UWB bandwidth (3.1 to 10.6 GHz) [5]. But such filters suffer from the spurious (higher order harmonics) behavior that results in narrow upper stop-band. Also these filter designs have some challenges regarding their compactness, consistent performance at frequencies of interest, cost of material and design complexities.

To reduce the size of UWB BPF's many techniques are reported some of which are defected ground structure [6–8], multilayer circuit [9, 10] and surface coupled structures [11]. These techniques have shown satisfactory performance in the desired pass band. Multilayer circuits face difficulty in integration with planar circuits along with constraints imposed by portable device for compact size and low insertion loss, therefore these UWB BPF's are not preferred. The aim of this paper is to present a novel UWB filter using combination of SIR, STER and contiguous SRR structure which provides UWB pass-band characteristics with multi-band notches. We have used CST microwave studio for parametric analysis.

2. FILTER CONFIGURATION AND ANALYSIS

The configuration of the proposed UWB filter is shown in Figure 1 Presented BPF consist combination of symmetrically tapered elliptical rings (STER) with vias and contiguous split ring resonators (SRR), in addition with stepped impedance resonator (SIR) structure, to realize the UWB pass band characteristics along with multi-band notches.

The dielectric material used for the design is RT/Duroid 5880 substrate with $\varepsilon_r = 2.2$ and thickness of 0.787 mm. In addition, we also aim to design the filter without modifications in ground plane. The dimensional configuration of proposed filter is explained in two parts (Part A and Part B). Part A explains SIR configuration and Part B explains about STER with contiguous SRR configuration The UWB band pass filter response is realized through a combination of low pass filter (LPF) and high pass filter (HPF) characteristics

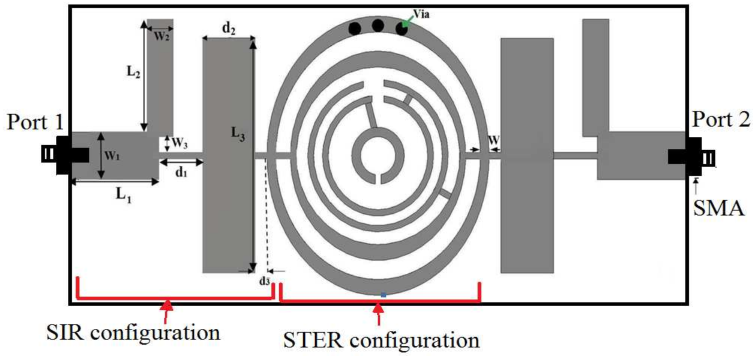

Figure 1. Proposed multi-band notch UWB band pass filter.

in order to produce a common pass band, which covers the entire UWB frequency range. The LPF ($f_H = 10.6\,\text{GHz}$) characteristics are realized through SIR configuration and the HPF ($f_L = 3.1\,\text{GHz}$) characteristics are achieved through vias in the STER configuration. The multi-notch bands are introduced over the UWB frequency band by integrating split rings in STER configuration (Figure 1) The input and output terminations are $50\,\Omega$, provided by a transmission line of width $W_1 = 1.8\,\text{mm}$.

2.1. Part A: SIR Configuration

For low pass characteristics in UWB bandwidth a conventional SIR method is used [12]. The initial stage of stepped impedance is modeled using a series and parallel combination of L's and C's for achieving a low pass filter response.

A low pass characteristic is obtained using a stepped impedance configuration along with open stub line as shown in Figure 2 In the equivalent SIR model, fringing capacitance (C_{fL}, Equation (4)) and inductance (L_{fc}, Equation (6)) are also considered to improve model's accuracy [12]. Parameters for SIR model are calculated as [13]:

$$C_{\mathit{eff}} = \frac{1}{Z_4 \omega_c} \tan\left(\frac{2\pi L_2}{\lambda_d}\right) \tag{1}$$

$$L_{\mathit{eff}} = \frac{Z_2}{\omega_c} \sin\left(\frac{2\pi d_1}{\lambda_d}\right) \tag{2}$$

$$L_e = \frac{Z_2}{\omega_c} \sin\left(\frac{2\pi d_3}{\lambda_d}\right) \tag{3}$$

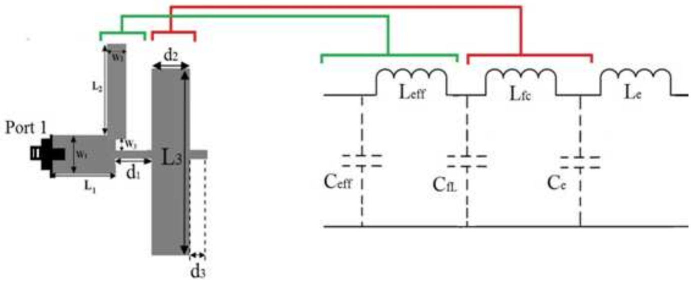

Figure 2. Equivalent circuit model of input stepped impedance stage. The dimensions of the SIR structure (Part A) is $W_1 = 1.8\,\mathrm{mm}$, $W_2 = 0.8\,\mathrm{mm}$, $W_3 = 0.4\,\mathrm{mm}$, $d_1 = 1.5\,\mathrm{mm}$, $d_2 = 1.5\,\mathrm{mm}$, $d_3 = 0.4\,\mathrm{mm}$, $L_2 = 3.9\,\mathrm{mm}$ and $L_3 = 7.2\,\mathrm{mm}$.

$$C_{fL} = \frac{1}{Z_2\omega_c}\tan^{-1}\left(\frac{\pi d_1}{\lambda_d}\right) \tag{4}$$

$$C_e = \frac{1}{Z_3\omega_c}\sin\left(\frac{2\pi d_2}{\lambda_d}\right) \tag{5}$$

And

$$L_{fc} = \frac{Z_3}{\omega_c}\tan^{-1}\left(\frac{\pi d_2}{\lambda_d}\right) \tag{6}$$

Where

$$\lambda_d = \frac{\lambda_c}{\sqrt{\varepsilon_{reff}}} \tag{7}$$

$$\varepsilon_{reff} = \frac{\varepsilon_r + 1}{2} + \frac{\varepsilon_r - 1}{2}\left(1 + 10\frac{h}{w}\right)^{-1/2} \tag{8}$$

Here 'h' is height of the substrate and 'w' is width of corresponding lines ($w/h > 1$) [13]. In above equations the values of Z_2 and Z_3 represents characteristic impedance of corresponding low and high impedance microstrip lines in SIR configuration Z_4 is the characteristic impedance of open-stub line and 'λ_d' is the guided wavelength at ω_c (cut-off frequency of LPF) For the equivalent model of Part A, the effective lumped inductors and capacitors values are given in Table 1. The upper cut-off frequency ($f_H = \omega_c = 10.6\,\mathrm{GHz}$) of UWB pass band is achieved by a combination of shunt stub ($L_2 \times W_2$) and SIR containing alternate high impedance ($d_1 \times (W_1 - 2W_3)$ microstrip line) and low impedance ($d_2 \times L_3$ microstrip line) sections [13]. The simulated low pass response of SIR configuration can be seen in Figure 3.

Table 1. Components of equivalent circuit.

Z_2	Z_3	Z_4	C_{eff}	C_{fl}	C_e	L_{eff}	L_{fc}	L_e
110 Ω	22 Ω	65 Ω	0.29 pF	1.568 fF	0.438 pF	1.35 nH	0.154 nH	0.563 nH

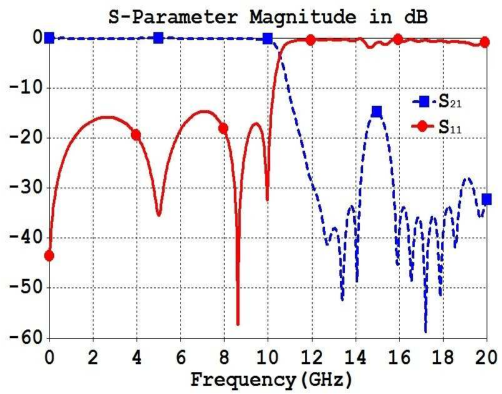

Figure 3. Low pass response of SIR configuration.

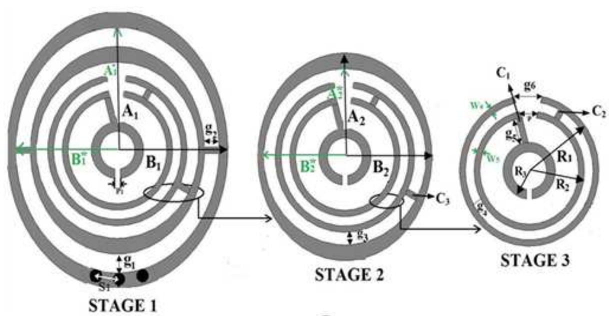

Figure 4. Symmetrically tapered elliptic rings (STER) along with contiguous SRR (Part B).

2.2. Part B: Configuration of Symmetrically Tapered Elliptical Rings (STER) along with Contiguous Split Ring Resonators (SRR)

To obtain a band notch characteristic in UWB response, a combination of STER and SRR is used, as shown in Figure 4. Elliptically-tapered rings are designed by removing an elliptical ring (major and minor axial radii as (A^*) and (B^*) respectively) from the slightly bigger ellipse (major and minor axial radii as (A) and (B) respectively). As both ellipse are concentric, $(A - A^*) > (B - B^*)$ configuration makes it symmetrically tapered structure. The proposed STER and SRR configuration have following dimensions (Figure 4): $A_1 = 4.4\,\text{mm}$, $B_1 = 3.8\,\text{mm}$, $A_1^* = 3.9\,\text{mm}$, $B_1^* = 3.5\,\text{mm}$, $A_2 = 3.3\,\text{mm}$, $B_2 = 3.0\,\text{mm}$, $A_2^* = 2.8\,\text{mm}$, $B_2^* = 2.8\,\text{mm}$, $g_1 = 0.6\,\text{mm}$, $g_2 = 0.5\,\text{mm}$, $g_3 = 0.4\,\text{mm}$, $g_4 = 0.5\,\text{mm}$, $g_5 = 1.0\,\text{mm}$, $g_6 = 0.7\,\text{mm}$, $R_1 = 2.4\,\text{mm}$, $R_2 = 1.9\,\text{mm}$, $R_3 = 0.9\,\text{mm}$, $W_4 = 0.22\,\text{mm}$, $W_5 = 0.25\,\text{mm}$, $P_1 = 0.3\,\text{mm}$, $S_1 = 0.1\,\text{mm}$ and $P = 0.4\,\text{mm}$.

STER is designed in order to produce good insertion loss at high frequencies of UWB pass band and also to improve the upper stop

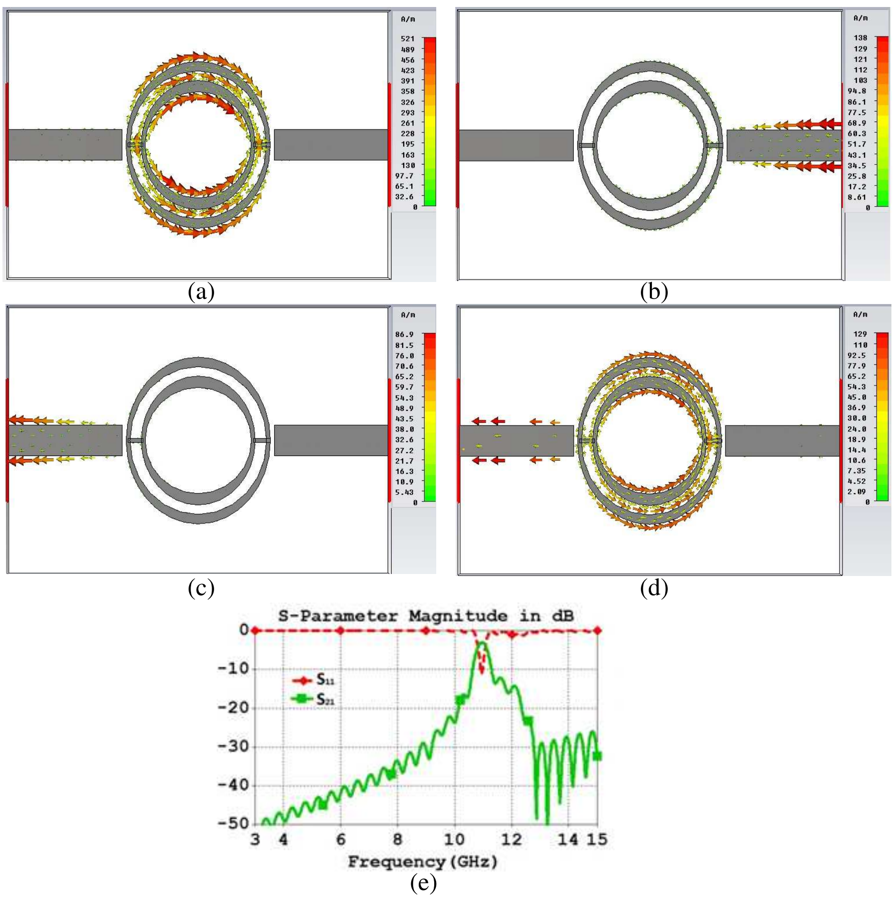

Figure 5. Current distribution in STER at (a) 10.8 GHz, (b) 8 GHz, (c) 4 GHz, (d) 12 GHz and (e) S-parameters of the symmetrically coupled STER.

band characteristics of the proposed filter. As shown in Figures 5(a)–(d) magnitude of current is more along STER at 10.8 GHz (Figure 5(a)) compare to other frequencies. The same resonant behavior is verified by S-parameters of the coupled STER as shown in Figure 5(e).

The behavior of STER and contiguous SRR is explained by its transmission line equivalent circuit model [14], as shown in Figure 6. The equivalent circuit model depicts STAGE 1 and STAGE 2 (Figure 4) of STER (L, C, L_a and L_b) along with STAGE 3 comprising contiguous SRR section (C_R and L_R) which is modeled as a resonant tank circuit responsible for band notches The passive components of lumped equivalent model of STAGE 3 depend on the orientation of contacts (C_1, C_2 and C_3) in contiguous SRR section as shown in Figure 7. The notch bands can be adjusted by changing the orientation of split rings or by changing positions of contacts (tapping positions) C_1, C_2 and C_3. The variations in position of C_3 are shown in Figure 7(b).

Figure 8 depicts Transmission characteristic ($|S_{21}|$) for different positions of contact line C_3. The angular position of contact C_3 is varied with respect to x-axis (clockwise) at 45° (Case 1), 90° (Case 2) and 135° (Case 3), while other contacts (C_1 and C_2) were kept at their initial positions (Figure 4).

The rotation of C_3 changes the tapping positions(contacts) of contiguous SRR section, that leads to change in electrical lengths between open ends of contiguous SRRs and C_3. This changes the band notch characteristics of proposed filter. Orientation of the contact strip does not change the equivalent tank circuit model, though it will

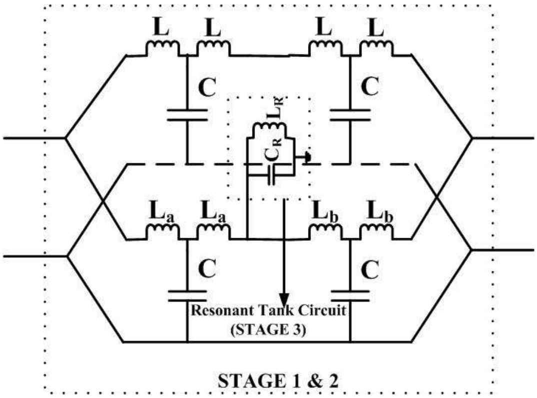

Figure 6. Equivalent model for Stages 1, 2 and 3 (STER configuration without vias).

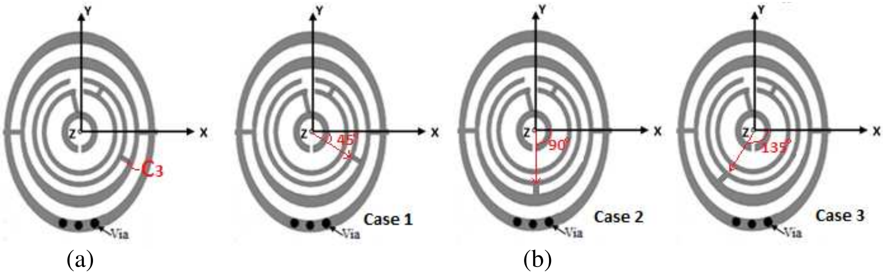

Figure 7. Spilt Ring contact C_3 at different positions: Case $1 = 45°$, Case $2 = 90°$ and Case $3 = 135°$ (clockwise with x-axis).

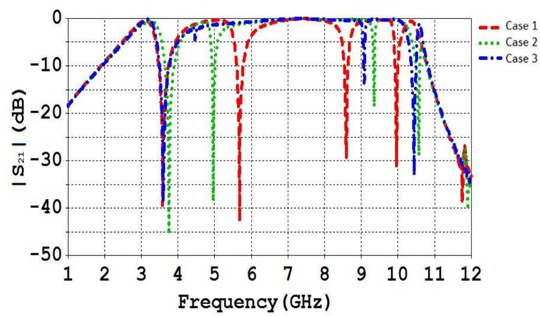

Figure 8. Transmission characteristic $|S_{21}|$ for positions of contact C_3.

have effect upon the equivalent L_R and C_R parameters as shown in Equation (9).

$$f_{nc} = \frac{1}{2\pi\sqrt{L_R \times C_R}} = \frac{C}{4L_{nc}\sqrt{\varepsilon_{reff}}} \tag{9}$$

Here 'f_{nc}' is the centre frequency of notch-band and L_{nc} effective resonant path length, and its value is given as:

$$L_{nc} \approx \frac{\lambda_g}{4} \tag{10}$$

λ_g is the guided wavelength for that particular notch frequency.

Band notch behavior for case 1, 2 or 3 can also be explained through current distributions. For Case 1, i.e., when C_3 is oriented 45° from X-axis (clock wise), band-notches (Figure 8 Case 1) are at 3.5–3.75 GHz, 5.5–5.8 GHz, 8.55–8.7 GHz and 9.89–10 GHz. Current distributions for center frequencies of respective notch-bands are shown in Figure 9. It can be seen in Figures 9(a)–(d) that, the dominance of current across some parts of contiguous SRRs is more (based on its resonant electrical length) for that particular notch frequency. For instance, at 3.6 GHz the magnitude of current is more along the path from C_3 to the open end of inner spilt ring in contiguous SRR section (via contact C_2, middle split ring and contact C_1) as shown in Figure 9(a). Similarly for 5.7 GHz, the magnitude of current is more along the path from C_3 to the open end of outer split ring of the SRR section as shown in the Figure 9(b). In same way Figure 9(c) and Figure 9(d) depicts the band notch characteristics via current distributions for 8.4 GHz and 9.95 GHz respectively. For other two cases (Case 2 and Case 3), similar nature of current distribution were observed at respective notch frequencies.

The positions of C_2 and C_1 (similar to C_3) can be adjusted to get the band-notches at different positions. This can be observed from the transmission characteristics of C_2 and C_1 orientations are shown in Figure 10(a) and Figure 10(b) respectively. Where C_2 and C_1 are angularly rotated (with respect to center of SRR section) clockwise and anti-clockwise from Y axis respectively, with orientations of 45° (Case 1), 90° (Case 2) and 135° (Case 3). In the same way band-notches for required frequencies can be achieved by changing the positions (angular orientation with respect to center of the contiguous SRR) of contacts individually or any combination of two or three contacts (C_1, C_2 and C_3) simultaneously. The notch-band width for different cases are tabulated in Table 2.

Table 2. Tabulated 10 dB notched bandwidth (GHz) (within UWB) for different cases.

	Notch Bandwidth Case 1 (45°)	Notch Bandwidth Case 2 (90°)	Notch Bandwidth Case 3 (135°)
C_3	3.5–3.8 5.5–5.8 8.55–8.7 9.89–10	3.65–5.85 4.9–5.02 9.32–9.45 10.5–10.65	4–4.5 9.01–9.12 10.4–10.6
C_2	4.5–5 6.35–6.4 8.6–8.75 10.1–10.2	4–4.4 5.9–6.1 8.5–8.6 10.1–10.15	3.5–3.8 5.9–6.1 8.2–8.35 10–10.12
C_3	3.4–3.85 5.6–5.75 9.5–9.6 (8 dB) 10.2–10.3	3.47–3.9 5.6–5.75 9.1–9.18 10–10.1	3.48–3.95 5.6–5.75 8.81–8.98 10.1–10.17

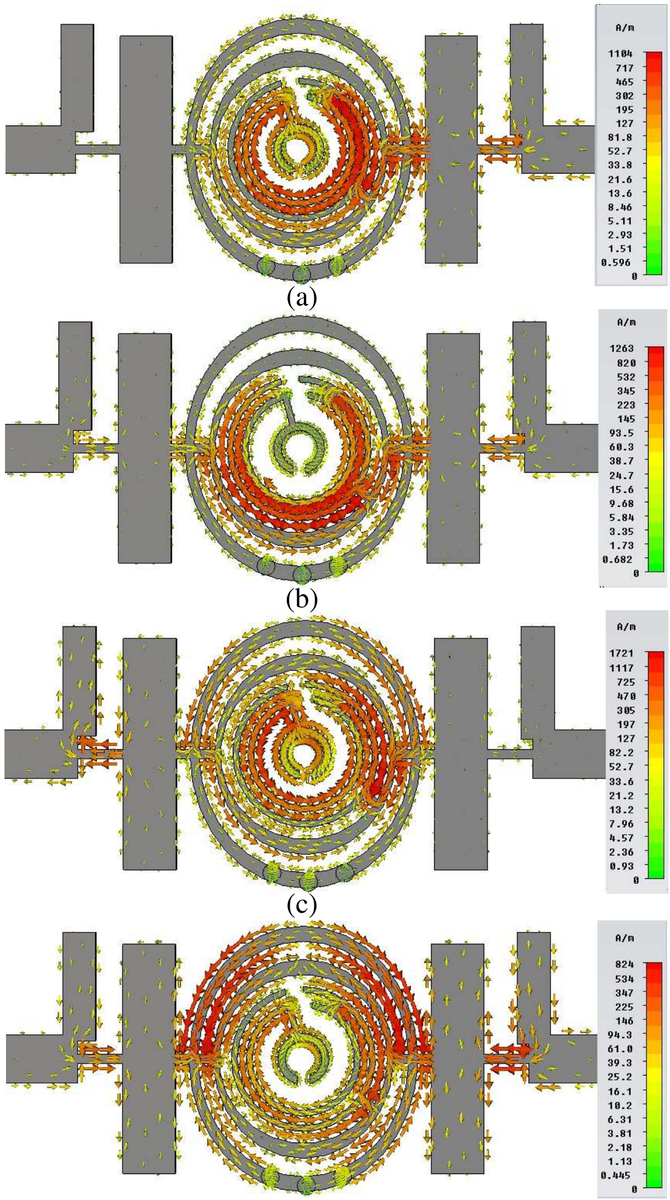

Figure 9. Current distribution (C_3 — Case 1) for center frequency of notch-band (f_{nc}) (a) 3.6 GHz, (b) 5.7 GHz, (c) 8.4 GHz and (d) 9.95 GHz.

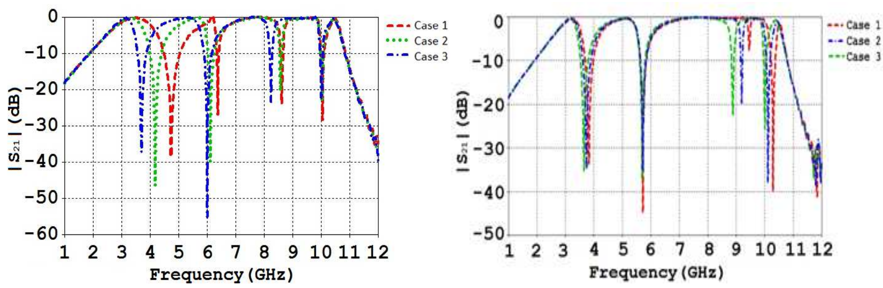

(a) (b)

Figure 10. Transmission characteristics ($|S_{21}|$) for orientation of contact positions of (a) C_2 and (b) C_1 for Case 1 (45°), Case 2 (90°), Case 3 (135°).

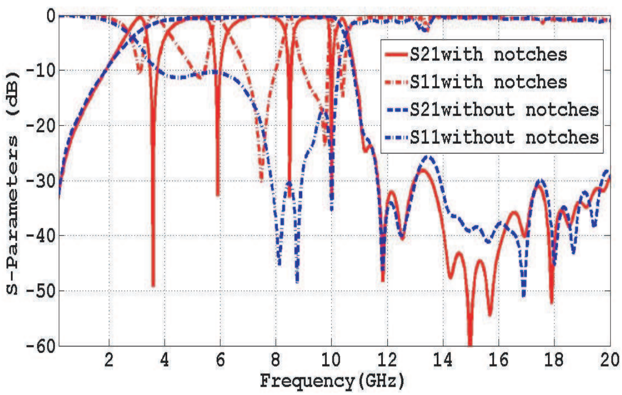

Figure 11. UWB pass band characteristics with and without band notch.

After analyzing band notch for different cases, a comparison between the response of proposed UWB filter (with and without notch characteristic) is shown in Figure 11. Based on simulated results and optimized dimensions (for required band pass and band stop characteristic) a prototype UWB BPF is fabricated.

3. MEASUREMENT AND ANALYSIS

As shown in Figure 12, the proposed UWB BPF is fabricated, for which the dimensions were optimized in order to produce UWB band pass response with desired band-notches. The optimized filter structure was implemented on RT/Duriod 5880 substrate with dielectric constant 2.2 and thickness 0.787 mm. The total surface dimension (exclusive of 50 Ω transmission line part) is $18 \times 12\,\mathrm{mm}^2$.

The optimized filter structure was implemented on RT/Duriod 5880 substrate with dielectric constant 2.2 and thickness 0.787 mm. The total surface dimension (exclusive of 50 Ω transmission line part) is $18 \times 12\,\mathrm{mm}^2$. Other dimensional configurations like tapping positions of the contacts ($C_1 = 110°$, $C_2 = 80°$ anticlockwise and $C_3 = 42°$ clockwise with respect to X-axis) were also adjusted in order to produce required band notches for co-existing narrow band services over the UWB band, i.e., WiMAX (3.4–3.6 GHz), WLAN (5.1–5.8 GHz), X-band applications like satellite communications and radar systems (8.4 GHz and 10 GHz).

The return loss and insertion loss were measured using Agilent Vector Network Analyzer (8722ET PNA). Analysis of fabricated prototype is done based on its reflection and insertion loss characteristic. Figure 13 shows the comparison between measured and simulated S_{21} and S_{11} characteristics. It can be seen that simulated and measured results with corresponding band-notch characteristics are in close agreement, but attenuation level of measured results at notch frequencies is less compared to simulated results. This response could have resulted from non-idealities of fabrication tolerances and losses in SMA connectors.

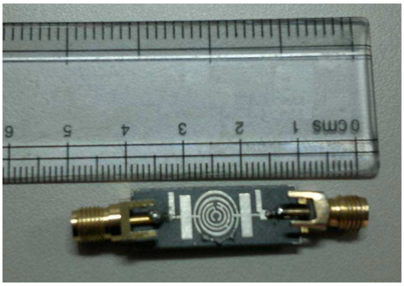

Figure 12. Fabricated UWB BPF prototype with dimentions as: $W_1 = 1.8\,\mathrm{mm}$, $W_2 = 0.8\,\mathrm{mm}$, $W_3 = 0.4\,\mathrm{mm}$, $d_1 = 1.5\,\mathrm{mm}$, $d_2 = 1.5\,\mathrm{mm}$, $d_3 = 0.4\,\mathrm{mm}$, $L_2 = 3.9\,\mathrm{mm}$, $L_3 = 7.2\,\mathrm{mm}$, $A_1 = 4.4\,\mathrm{mm}$, $B_1 = 3.8\,\mathrm{mm}$, $A_1^* = 3.9\,\mathrm{mm}$, $B_1^* = 3.5\,\mathrm{mm}$, $A_2 = 3.3\,\mathrm{mm}$, $B_2 = 3.0\,\mathrm{mm}$, $A_2^* = 2.8\,\mathrm{mm}$, $B_2^* = 2.8\,\mathrm{mm}$, $g_1 = 0.6\,\mathrm{mm}$, $g_2 = 0.5\,\mathrm{mm}$, $g_3 = 0.4\,\mathrm{mm}$, $g_4 = 0.5$, $g_5 = 1.0\,\mathrm{mm}$, $g_6 = 0.7\,\mathrm{mm}$, $R_1 = 2.4\,\mathrm{mm}$, $R_2 = 1.9\,\mathrm{mm}$, $R_3 = 0.9\,\mathrm{mm}$, $W_4 = 0.22\,\mathrm{mm}$, $W_5 = 0.25\,\mathrm{mm}$, $P_1 = 0.3\,\mathrm{mm}$, $S_1 = 0.1\,\mathrm{mm}$ and $P = 0.4\,\mathrm{mm}$.

The measured result shown in Figure 13 depicts that, proposed filter exhibits UWB BPF response. The pass bands for which insertion loss is less than 3 dB are 2.8–3.2 GHz, 3.9–5.5 GHz, 6.12–8.2 GHz and 9.62–10.6 GHz. The corresponding fractional bandwidths are 5%, 20.75%, 27.01% and 11.425%. The insertion loss and return loss for simulated and measured band notch characteristics of the proposed filter are listed in Table 3.

The performance of the presently proposed structure along with the parameters of other UWB BPFs is compared in Table 4. The results show that presented work has advantages of adjustable multi-notches (four) and compact size.

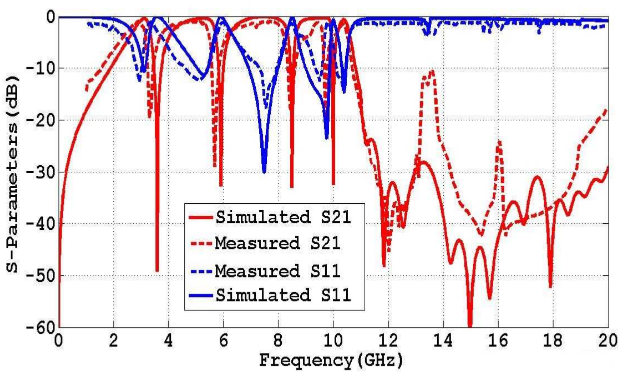

Figure 13. Simulated and measured S-parameter results of proposed UWB BPF.

Table 3. Comparison of simulated and measured band notch characteristics of the proposed filter.

	Simulated Results		Measured Results	
Notch Frequencies (GHz)	Return Loss S_{11} (dB)	Insertion Loss S_{21} (dB)	Return Loss S_{11} (dB)	Insertion Loss S_{21} (dB)
3.6	−0.12	−49	−1.33	−19.5
5.7	−0.21	−34	−1.03	−29.04
8.4	−0.3	−35.2	−1.98	−18.14
9.9	−0.4	−34.3	−2.19	−17.89

Table 4. Comparison of proposed work with various UWB BPFs (N/A = Not Applicable).

Parameters \References	Proposed work	[15]	[16]	[17]	[18]	[19]	[20]
Permittivity (ε_r)	2.2	2.2	2.65	4.4	2.2	2.2	4.4
Thickness (mm)	0.787	1.0	0.8	0.8	1.0	0.787	0.8
Number of notches	4 (variable)	3	N/A	2	2	2	2
Notch frequency/ Attenuation level in dB	3.6/19, 5.8/28, 8.5/18 and 10/17	5.2, 5.85 and 8.0/>10	N/A	3.5 and 5.8 / >15	5.85 and 8.0 / >15	4.8 and 8/ >10	5.45 and 6.3 / >14
3–dB band width (GHz)	3-10.8	2.8-11.0	3-10.5	2.8-9.6	2.8-10.9	2.8-11.0	3.1-10.6
Size (mm^2)	18×12	30.6×20	10×3.2	11×10.5	34×20	23.6×2.7	20×12
Publication year	-	2012	2012	2010	2011	2010	2010

4. CONCLUSION

A compact printed UWB BPF with combination of SIR and STER with contiguous SRR configuration is designed, fabricated and measured. The measured results depicts a good multi-band notched UWB filter characteristics with insertion loss less than 1.2 dB in pass band and more than 17 dB at the center frequencies of notched bands. A novel technique proposed in this paper is implementation of band notches in the UWB band by introducing adjustable contiguous SRR. In present structure STER with vias and SIR are used to improve the band pass characteristics of the proposed filter. The notch bands positions can be controlled by changing the location of contact C_1, C_2 and C_3. The contact positions (C_1, C_2 and C_3) in contiguous SRR section are optimized in order to avoid interference caused by the WiMAX, WLAN and X-band applications. The proposed configuration can also be made programmable by adjusting the positions of C_1, C_2 and C_3 on the filter. Therefore proposed filter is suitable to design reconfigurable band notch UWB filter, to provide immunity from interference, caused due to co-existing narrow band services and upcoming new wireless technologies.

REFERENCES

1. FCC, Revision of Part 15, the Commission's Rules Regarding to Ultra-Wide-Band Transmission System, First Note and Order Federal Communication Commission, ET-Docket, 98–153, 2002.
2. Sarkar, P., R. Ghatak, M. Pal, and D. R. Poddar, "Compact UWB bandpass filter with dual notch bands using open circuited stubs," *IEEE Microwave and Wireless Components Letters*, Vol. 22, No. 9, Sept. 2012.
3. Wei, F., W. T. Li, X. W. She, and Q. L. Huang "Compact UWB bandpass filter with triple-notched bands using triple-mode stepped impedance resonator," *IEEE Microwave and Wireless Components Letters*, Vol. 22, No. 10, 512–514, Oct. 2012.
4. Sarkar, P., R. Ghatak, and D. R. Poddar, "A compact UWB bandpass filter with multiple notch band using open circuited stub," *IEEE Applied Electromagnetics Conference (AEMC)*, Dec. 18–22, 2011.
5. Lee, C.-H., I.-C. Wang, and L.-Y. Chen, "MMR-based band-notched UWB bandpass filter design," *Journal of Electromagnetic Waves and Applications*, Vol. 22, Nos. 17–18, 2407–2415, 2008.
6. Gao, S. S., S. Q. Xiao, J. P. Wang, X. S. Yang, Y. X. Wang, and B. Z. Wang, "A compact UWB bandpass filter with wide stopband," *Journal of Electromagnetic Waves and Applications*, Vol. 22, Nos. 8–9, 1043–1049, 2008.
7. Wei, F., P. Chen, L. Chen, and X. W. Shi, "Design of a compact UWB bandpass filter with wide defected ground structure," *Journal of Electromagnetic Waves and Applications*, Vol. 22, No. 13, 1783–1790, 2008.
8. Fallahzadeh, S. and M. Tayarani, "A new microstrip UWB bandpass Filter using defected microstrip structure," *Journal of Electromagnetic Waves and Applications*, Vol. 24, No. 7, 893–902, 2010.
9. Packiaraj, D., K. J. Vinoy, and A. T. Kalghatg, "Analysis and design of two layered ultra wide band filter," *Journal of Electromagnetic Waves and Applications*, Vol. 23, Nos. 8–9, 1235–1243, 2009.
10. Hao, Z. C. and J. S. Hong, "Compact UWB filter with double notch-bands using multiplayer LCP technology," *IEEE Microwave and Wireless Components Letters*, Vol. 19, No. 8, 500–502, Aug. 2009.
11. Huang, J.-Q., Q.-X. Chu, and C.-Y. Liu, "Compact UWB filter based on surface-coupled structure with dual notched bands,"

Progress In Electromagnetics Research, Vol. 106, 311–319, 2010.
12. Fooks, E. H. and R. A. Zakareviius, *Microwave Engineering Using Microstrip Circuits*, *Prentice Hall*, Technology and Engineering, 1990.
13. Pozar, D. M., *Microwave Engineering*, 2nd Edition, John Wiley & Sons, Inc., 1998.
14. Chang, K. and L.-H. Hsieh, *Microwave Ring Circuits and Related Structures*, 2nd Edition, John Wiley & Sons, Inc., 2004.
15. Li, R. and L. Zhu, "Compact UWB bandpass filter using stub-loaded multiple-mode resonator," *IEEE Microwave and Wireless Components Letters*, Vol. 17, No. 1, 40–43, Jan. 2007.
16. Wang, H., Y. Y. Zheng, W. Kang, C. Miao, and W. Wu, "UWB bandpass filter with novel structure and super compact size," *Electronics Letters*, Vol. 48, No. 17, Aug. 16th, 2012.
17. Wei, F., Q. Y. Wu, X. W. Shi, Senior, and L. Chen, "Compact UWB bandpass filter with dual notched bands based on SCRLH resonator," *IEEE Microwave and Wireless Components Letters*, Vol. 21, No. 1, 28–30, Jan. 2011.
18. Hsiao, P.-Y. and R.-M. Weng, "Compact tri-layer ultra-wideband band-pass filter with dual notch bands," *Progress In Electromagnetics Research*, Vol. 106, 49–60, 2010.
19. Song, K. and Q. Xue, "Compact ultra-wideband (UWB) bandpass filters with multiple notched bands," *IEEE Microwave and Wireless Components Letters*, Vol. 20, No. 8, 447–449, Aug. 2010.
20. Hsiao, P.-Y. and R.-M. Weng, "Compact open-loop UWB filter with notched band," *Progress In Electromagnetics Research Letters*, Vol. 7, 149–159, 2009.